CHAPTER 6

A Modulation Method for the Power-Line Communication Channel

As we have seen in previous chapters the power-line channel is a harsh environment. The characteristics of the channel tend to vary in time, location and with different loads. The study in Chapter 2 describes this behavior.

One possible solution to overcome the problems with such a channel, is to use a robust modulation method. Furthermore, if the modulation method is able to handle unknown attenuation and unknown phase shifts, then the receiver can be simplified. The problem is to combine these requirements with the high bit rate needed in today's computer communications and the bandwidth limitation on the power-line channel.

The intention with this chapter is to present a modulation that may be a candidate to be used in a communication system for the power-line channel. Here, the focus is on the error probability properties, for the considered set of uncoded information carrying signals, when these are detected non-coherently. In a practical system (coded) these signals might be combined with a chosen encoder and interleaver structure. This is also discussed in the end of this chapter, using known properties of the power-line channel.

The disposition of the chapter is as follows:

Section 6.1 gives a general description of the modulation method. Section 6.2 shows computer-simulated results of the performance of the method and Section 6.3 theoretically validates the simulations. In Section 6.4 we combine the method with coding, diversity and the use of sub-bands. Finally Section 6.5 concludes the results.

6.1 The Modulation Method

Figure 6-1 shows a model of the communication system considered in this chapter, [1], [41], [54]. The transmitter transmits a signal, $s(t)$, on the channel, which is modeled as a

time-variant linear filter *H(f,t)*. The noise at the receiver, *N*(*t*), is modeled as AWGN (Additive White Gaussian Noise).

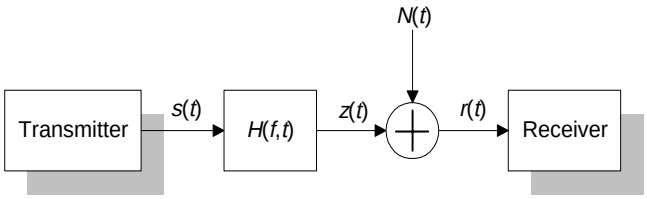

FIGURE 6-1 A model of the communication system.

The sequence of information bits have bit rate R_b b/s and the number of signal alternatives (also symbols), are denoted *M*, thus the symbol rate is $R_b/\log_2 M$ b/s. The bandwidth of the system is denoted *W* and it is assumed that the attenuation in this region is constant. *W* can here be interpreted as, e.g., a single sub-channel in an OFDM-type of arrangement. It is also assumed that the attenuation and the phase shift of the channel are unknown. Other important parameters are the symbol time $T_s=1/R_s$ and the bit time $T_b=1/R_b$, which defines the time needed for transmitting a symbol and a bit respectively.

Two modulation methods often used are orthogonal FSK (Frequency Shift Keying) and PSK (Phase Shift Keying) [41]. FSK (when non-coherently detected) is a robust method that works even when the phase and the attenuation are unknown. However, the attenuation must be constant within the communication bandwidth, which is assumed in this chapter. A disadvantage with FSK is that the bandwidth efficiency is low. Figure 6-2 shows the estimated bandwidth, *W*, of a FSK modulated signal with *M* signal alternatives. It is here assumed that the hcs (Half Cycle Sinusoidal) [41] pulse is used. The double sided mainlobe bandwidth (about 99.5% of the power) of this pulse is $3R_s$ and the frequency separation needed in this case to obtain orthogonality is $2R_s$ (other pulse-shapes are possible). Because each symbol is associated with a certain frequency the bandwidth will be large for large *M*.

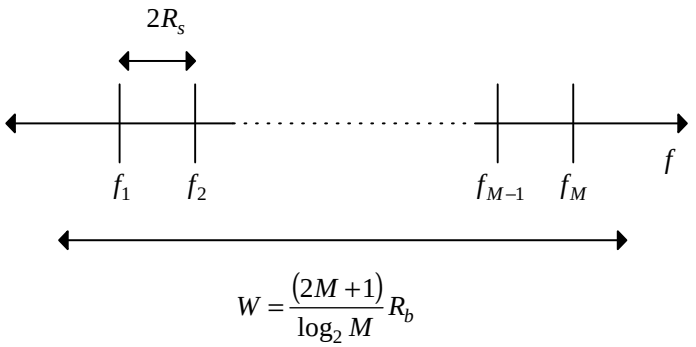

FIGURE 6-2 The estimated bandwidth of a FSK signal.

For pure PSK, the information is modulated in the phase (only one carrier is used) and thus it fails if the unknown phase, which is introduced by the channel, is not compensated for in the receiver. Figure 6-3 shows the estimated bandwidth of a PSK signal. Also here it is assumed that the hcs pulse is used. The bandwidth decreases when M increases (for a fixed R_b), thus the bandwidth efficiency increases with increasing number of symbols.

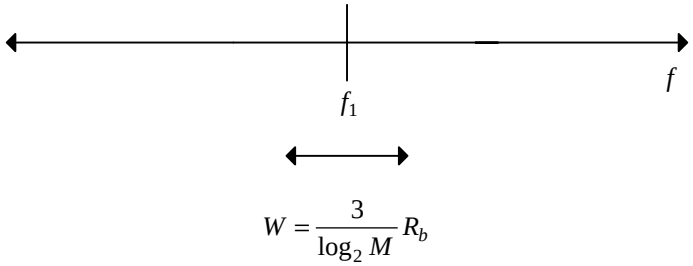

FIGURE 6-3 The estimated bandwidth of a PSK signal.

An extension of PSK, DPSK (Differential Phase Shift Keying) [41], [51] is sometimes used when the phase is unknown. The bandwidth efficiency of DPSK is high, the same as for PSK, but it requires the phase to be stable (or slowly varying) during at least two symbol intervals.

The modulation method investigated in this chapter is supposed to achieve robustness, a variety of bandwidth efficiencies and ease of implementation. It is designed to handle, to a certain extent, unknown attenuation and phase shifts. The method consists of one FSK modulated signal (with M_0 signal alternatives) and J PSK modulated signals, where each PSK signal is allowed to have an arbitrary number of signal alternatives. The use of the FSK signal is two-fold. It carries information, and it is also used in the receiver to estimate the received phase in the PSK signal. Because the receiver is not dependent on the attenuation and the phase of the channel, within the frequency band W, the system will work on channels where the attenuation and the phase shifts are unknown. Figure 6-4 shows the estimated bandwidth of the modulation method.

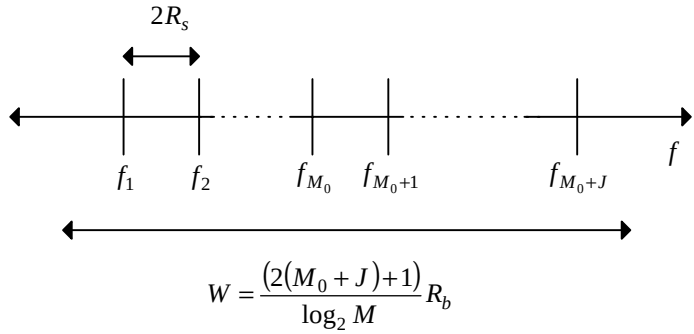

FIGURE 6-4 The estimated bandwidth of the proposed modulation method.

In the following sections each part of the communication system is described.

6.1.1 The Transmitter

The transmitter is shown in Figure 6-5. ***b*** is the sequence of information bits having bit rate $R_b=1/T_b$ bps. The bits are converted into one or more bit streams $\{\boldsymbol{b_0}, \boldsymbol{b_1}, ...\boldsymbol{b_J}\}$ by a serial to parallel converter and each stream is associated with one of the sub-modulation methods.

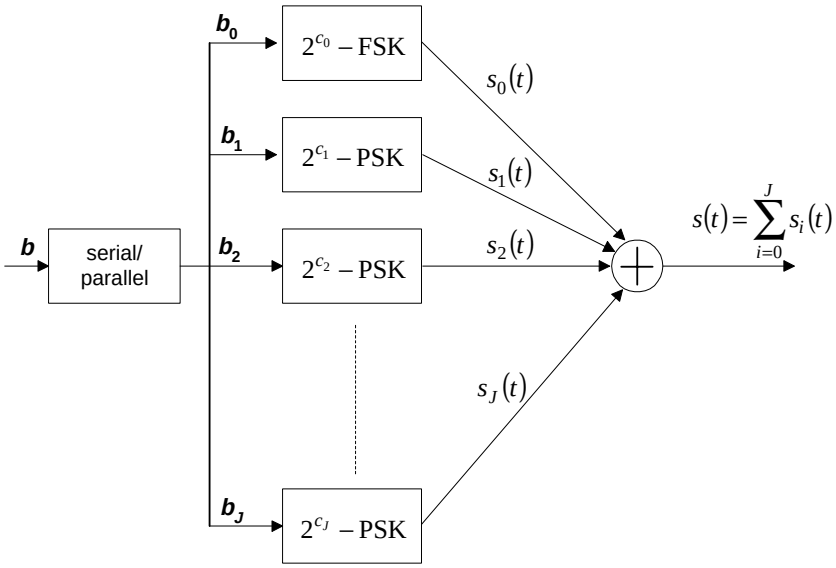

FIGURE 6-5 The transmitter.

A sub-modulation scheme, *i*, transmits c_i number of bits in each symbol interval, T_s, and thus has $M_i = 2^{c_i}$ different symbols or signals. In a symbol interval T_s, $c = \sum_{i=0}^{J} c_i$ bits are transmitted, hence the symbol rate equals $R_s=R_b/c$. The bit rate in each sub-sequence $\boldsymbol{b_i}$ equals c_iR_s and the total number of symbols is $M=2^c$.

In each symbol interval the signal $s(t)$ is the sum of the signals $\{s_0(t),.....,s_J(t)\}$ where

$$s_0(t) = \sum_{i=1}^{M_0} A_i g(t)\sqrt{2}\cos(2\pi f_i t + \varphi_{ref}),\ 0 \le t \le T_s \qquad (6\text{-}1)$$

where A_i is A or zero depending on the c_0-tuple of bits. Because $s_0(t)$ is a FSK signal only one of the M_0 frequencies is sent, so only one A_i may be non-zero.

The PSK-signals, $s_i(t)$, are described as,

$$s_i(t) = Bg(t)\sqrt{2}\cos(2\pi f_{M_0+i}t + \varphi_{ref} + \nu_i),\ 0 \le t \le T_s,\ i = 1, ..., J \qquad (6\text{-}2)$$

Depending on the c_i-tuple of bits, ν_i takes one of the phase values $\{\nu_{i,j}\}_{j=1}^{M_i}$. Hence, for i=1,2,....,J, $s_i(t)$ is an M_i-ary PSK signal with amplitude B and frequency f_{M_0+i}.

The reference phase, φ_{ref}, must be the same for all the (M_0+J) frequencies in the interval $0<t<T_s$. However, φ_{ref} is allowed to be different in different symbol intervals. The pulse-shape $g(t)$ is not specified but typically the half cycle sinusoidal (hcs) pulse may be used. The energy of $g(t)$, E_g, is assumed to be one and the frequency spacing is chosen such that an 2(M_0+J)-dimensional signal space is achieved, based on the M_0+J frequencies in (6-1) and (6-2).

As Figure 6-5 shows, a large number of different modulation systems may be described with this model. We will study three of the possible combinations:

- 2-FSK and 2-PSK. Denoted BB.
- 2-FSK and 4-PSK. Denoted BQ.
- 2-FSK, 2-PSK and 2-PSK. Denoted BBB.

The reason for choosing these specific schemes is their simple construction. We are trying to find alternative signal constellations, which eventually can be used combined with coding. Table 6-1 shows the bandwidth efficiency for the considered modulation systems compared to PSK and FSK (assuming the hcs pulseshape in all cases). As the table shows the bandwidth efficiency is better than FSK but smaller than PSK. This means that a larger amount of data can be transmitted with this system than with FSK, but to make a fair comparison it is needed to also consider the symbol/bit error probability.

M	**FSK**	**PSK**	**BB**	**BQ**	**BBB**
2	1/5	1/3	-	-	-
4	2/9	2/3	2/7	-	-
8	3/17	3/3	-	3/7	3/9

TABLE 6-1 The bandwidth efficiency for FSK, PSK and the investigated modulation methods.

6.1.2 Communication Channel

The model used for the communication channel is described in Section 1.3.6. It is here assumed that within the information signal bandwidth, W, the transfer function of the channel can be approximated as (see [23], [51])

$$H(f) = |H(f)|e^{j\beta(f)} \approx \alpha e^{j(\beta(f_c) - 2\pi(f - f_c)\tau_g)}, f_c - \frac{W}{2} \le f \le f_c + \frac{W}{2} \quad (6\text{-}3)$$

where $\alpha = |H(f_c)|$, τ_g is the group delay defined as $\tau_g = -\frac{1}{2\pi}\frac{\partial\beta(f)}{\partial f}\Big|_{f=f_c}$, $\beta(f_c)$ is the phase delay at the point $f=f_c$, and the center (or carrier) frequency $f_c = \frac{f_1 + f_{M_0+J}}{2}$. The attenuation is assumed constant within the communication bandwidth W and τ_g is assumed to be implicitly estimated by the receiver. It is assumed that W is small enough (T_s large enough) such that this model is valid. As a consequence, R_b must be low.

The noise is assumed to be AWGN [41] with double-sided power spectrum $N_0/2$.

6.1.3 The Receiver

The received signal, $r(t)$, (see Figure 6-1) in the first symbol interval, $\tau_g \le t \le \tau_g + T_s$, is

$$\begin{aligned} r(t) = {} & \alpha \sum_{i=1}^{M_0} A_i g(t - \tau_g)\sqrt{2}\cos(\omega_c t + \Delta\omega_i(t - \tau_g) + \varphi_{ref} + \beta(f_c)) + \\ & \alpha \sum_{i=1}^{J} Bg(t - \tau_g)\sqrt{2}\cos(\omega_c t + \Delta\omega_{M_0+i}(t - \tau_g) + \varphi_{ref} + \nu_i + \beta(f_c)) + N(t) \end{aligned} \quad (6\text{-}4)$$

where $\Delta\omega_i = 2\pi(f_i - f_c)$ and $\omega_c = 2\pi f_c$ [41]. Compare with (6-1) and (6-2).

To obtain a ML (Maximum Likelihood) receiver we first find the basis vectors. The receiver is then built of a parallel bank of crosscorrelators, which compute the projection of the received signal on each of the basis functions.

As basis functions for the signals we have (assuming the energy of the pulse $g(t)$ is one)

$$\begin{aligned} \phi_1(t) &= g(t - \tau_g)\sqrt{2}\cos(\omega_c t + \Delta\omega_i(t - \tau_g)), \tau_g \le t \le \tau_g + T_s \\ \phi_1(t) &= -g(t - \tau_g)\sqrt{2}\sin(\omega_c t + \Delta\omega_i(t - \tau_g)), \tau_g \le t \le \tau_g + T_s \end{aligned} \quad (6\text{-}5)$$

With trigonometric identities it can be shown that the correlation demodulator can be divided in two parts, first demodulation to baseband and then a set of filter banks.

The signal is demodulated to baseband by the block shown in Figure 6-6 and the responses to the signal $r(t)$ are

$$
\begin{aligned}
r_1(t) &= \alpha \sum_{i=1}^{M_0} A_i g(t-\tau_g)\cos(\Delta\omega_i(t-\tau_g) + \varphi_{ref} + \beta(f_c) - \varphi_d) + \\
&\quad \alpha \sum_{i=1}^{J} Bg(t-\tau_g)\cos(\Delta\omega_{M_0+i}(t-\tau_g) + \varphi_{ref} + \nu_i + \beta(f_c) - \varphi_d) + n_1(t) \\
r_2(t) &= \alpha \sum_{i=1}^{M_0} A_i g(t-\tau_g)\sin(\Delta\omega_i(t-\tau_g) + \varphi_{ref} + \beta(f_c) - \varphi_d) + \\
&\quad \alpha \sum_{i=1}^{J} Bg(t-\tau_g)\sin(\Delta\omega_{M_0+i}(t-\tau_g) + \varphi_{ref} + \nu_i + \beta(f_c) - \varphi_d) + n_2(t)
\end{aligned}
\tag{6-6}
$$

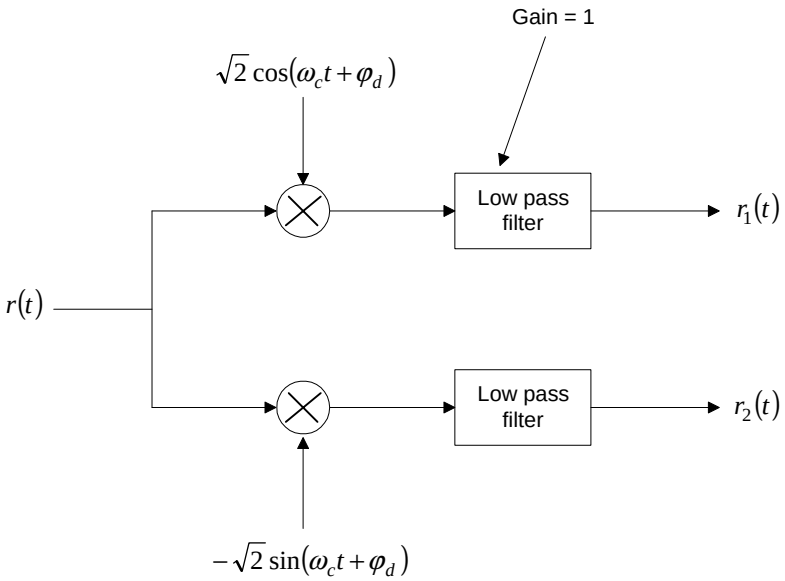

FIGURE 6-6 Demodulation to baseband.

The unknown phase φ_d is the introduced phase in the receiver. This allows an easy implementation of the receiver because no synchronisation is needed. A set of filterbanks is used to extract the decision variables. The filter bank for frequency f_1 is shown in Figure 6-7.

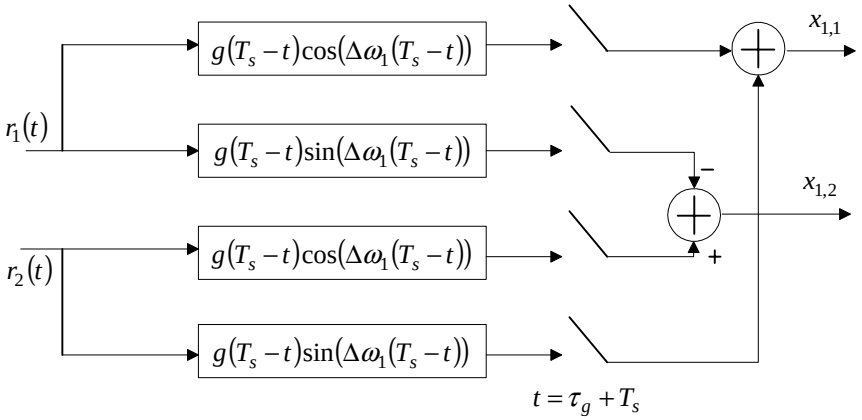

FIGURE 6-7 The filter bank for frequency f_1.

The responses to the filters in Figure 6-7 are:

$$x_{1,1} = \alpha A_1 E_g \frac{\cos(\theta)}{2} + n_{1,1} + \alpha A_1 E_g \frac{\cos(\theta)}{2} + n_{1,2} = \alpha A_1 E_g \cos(\theta) + W_{1,1} \tag{6-7}$$

$$x_{1,2} = \alpha A_1 E_g \frac{\sin(\theta)}{2} + n_{2,1} + \alpha A_1 E_g \frac{\sin(\theta)}{2} + n_{2,2} = \alpha A_1 E_g \sin(\theta) + W_{1,2} \tag{6-8}$$

where

$$\begin{aligned} \theta &= \varphi_{ref} + \beta(f_c) - \varphi_d \\ W_{1,1} &= n_{1,1} + n_{1,2} \\ W_{1,2} &= n_{2,1} + n_{2,2} \end{aligned} \tag{6-9}$$

Assuming that E_g=1 then $W_{1,1}$ and $W_{1,2}$ are independent Gaussian random variables with variance $N_0/2$ and mean zero.

If these calculations are repeated for $\Delta\omega_2 \ldots \Delta\omega_{M_0+J}$ then the set of complex decision variables obtained is:

$$\begin{aligned} X_i &= \alpha A_i e^{j\theta} + W_i,\ i = 1, 2, \ldots, M_0 \\ Y_i &= \alpha B e^{j\nu_i} e^{j\theta} + W_{i+M_0},\ i = 1,2,\ldots,J \end{aligned} \tag{6-10}$$

where

(6-11)

$$\begin{aligned} W_i &= W_{i,1} + jW_{i,2} \\ X_i &= x_{i,1} + jx_{i,2} \\ Y_i &= y_{i,1} + jy_{i,2} \end{aligned} \tag{6-12}$$

These M_0+J complex decision variables contain all information relevant to make a decision of which message was sent. In the equations j^2=-1.

6.1.4 The Maximum Likelihood Decision Rule

Define $\boldsymbol{r}$ as the set $\{x_{1,1}, x_{1,2}, ..., x_{M_0,1}, x_{M_0,2}, y_{1,1}, y_{1,2}, ..., y_{J,1}, y_{J,2}\}$. The ML (Maximum Likelihood) decision rule [41] finds the maximum of the probabilities $p(\boldsymbol{r}|m_l)$ assuming message l was sent. These probability density functions can be obtained by averaging the pdfs $p(\boldsymbol{r}|m_l,\theta)$:

$$p(\boldsymbol{r}|m_l) = \int_0^{2\pi} p(\boldsymbol{r}|m_l, \theta)p(\theta)d\theta \tag{6-13}$$

If we assume that the phase, θ, is uniformly distributed then $p(\theta) = \frac{1}{2\pi}$ in a 2π-interval. The probability $p(\boldsymbol{r}|m_l,\theta)$ can be expressed as a product of the marginal pdfs,

$$p(\boldsymbol{r}|m_l, \theta) = \prod_{i=0}^{M_0} (p(x_{i,1}|m_l, \theta)p(x_{i,2}|m_l, \theta)) \cdot \prod_{i=1}^{J} (p(y_{i,1}|m_l, \theta)p(y_{i,2}|m_l, \theta)) \tag{6-14}$$

Define A_k^l as the value of A_k for message number l and ν_k^l as the value of ν_k for message number l. Because the outputs from the filter banks are independent Gaussian random variables with variance $\sigma^2=N_0/2$ the pdfs may be written as

$$
\begin{aligned}
p(\mathbf{r}|m_l,\theta) &= \prod_{i=1}^{M_0} \frac{1}{2\pi\sigma^2}\exp\left(-\frac{\left(x_{i,1}-\alpha A_i^l\cos(\theta)\right)^2+\left(x_{i,2}-\alpha A_i^l\sin(\theta)\right)^2}{2\sigma^2}\right) \\
&\quad \prod_{i=1}^{J} \frac{1}{2\pi\sigma^2}\exp\left(-\frac{\left(y_{i,1}-\alpha B\cos\left(\nu_i^l+\theta\right)\right)^2+\left(y_{i,2}-\alpha B\sin\left(\nu_i^l+\theta\right)\right)^2}{2\sigma^2}\right) \\
&= \left(\frac{1}{2\pi\sigma^2}\right)^{M_0+J}\prod_{i=1}^{M_0}\exp\left(-\frac{x_{i,1}^2+x_{i,2}^2+\left(\alpha A_i^l\right)^2}{2\sigma^2}\right)\prod_{i=1}^{J}\exp\left(-\frac{y_{i,1}^2+y_{i,2}^2+(\alpha B)^2}{2\sigma^2}\right) \\
&\quad \prod_{i=1}^{M_0}\exp\frac{x_{i,1}\alpha A_i^l\cos(\theta)+x_{i,2}\alpha A_i^l\sin(\theta)}{\sigma^2}\prod_{i=1}^{J}\exp\left(\frac{y_{i,1}\alpha B\cos\left(\nu_i^l+\theta\right)+y_{i,2}\alpha B\sin\left(\nu_i^l+\theta\right)}{\sigma^2}\right)
\end{aligned}
\tag{6-15}
$$

The constants may be removed as they appear in all pdfs and integration yields

$$
\begin{aligned}
&\int_0^{2\pi}\prod_{i=1}^{M_0}\exp\frac{x_{i,1}\alpha A_i^l\cos(\theta)+x_{i,2}\alpha A_i^l\sin(\theta)}{\sigma^2} \\
&\prod_{i=1}^{J}\exp\frac{y_{i,1}\alpha B\left(\cos\left(\nu_i^l\right)\cos(\theta)-\sin\left(\nu_i^l\right)\sin(\theta)\right)+y_{i,2}\alpha B\left(\sin\left(\nu_i^l\right)\cos\theta+\cos\left(\nu_i^l\right)\sin\theta\right)}{\sigma^2}d\theta \\
&= I_0\left(\frac{\sqrt{R^2+S^2}}{\sigma^2}\right)
\end{aligned}
\tag{6-16}
$$

where

$$
\begin{aligned}
R &= \left(\sum_{i=1}^{M_0} x_{i,1}\alpha A_i^l+\sum_{i=1}^{J}\left(y_{i,1}\alpha B\cos\left(\nu_i^l\right)+y_{i,2}\alpha B\sin\left(\nu_i^l\right)\right)\right) \\
S &= \left(\sum_{i=1}^{M_0} x_{i,1}\alpha A_i^l-\sum_{i=1}^{J}\left(y_{i,1}\alpha B\sin\left(\nu_i^l\right)+y_{i,2}\alpha B\cos\left(\nu_i^l\right)\right)\right)
\end{aligned}
\tag{6-17}
$$

and $I_0(x)$ is the modified Bessel function of the zeroth order [23], [41]. Because the Bessel function is monotonously increasing the optimum decision rule maximizes

$$
\sqrt{R^2+S^2} \tag{6-18}
$$

α is a constant and can be removed from the expression so, in order to find the most probable transmitted symbol message, the detector calculates the set

$$C^l = \left| \sum_{i=1}^{M_0} X_i A_i^l + \sum_{i=1}^{J} Y_i B e^{-j\nu_i^l} \right|, 1 \le l \le M \qquad (6\text{-}19)$$

and chooses message m if $C^m = \max_i C^i$. In the noiseless case $C_{max} = A^2 + JB^2$.

6.2 Computer Simulations

In this section we evaluate, by computer simulations, the performance of the three modulation methods described in Section 6.1.1. The reason for choosing these specific schemes is their simple construction. The performance is estimated in terms of the symbol error probability and it is compared to non-coherent FSK and DPSK.

The phase is considered a uniformly distributed variable in the interval 0 to 2π and the signal alternatives are assumed to be equally likely. These parameters are randomly chosen by the simulation program.

The performance depends on the relation between the parameters *A* and *B*. Because the minimum euclidean distance is related to the symbol error probability, the relation between *A* and *B* is chosen such that the minimum Euclidean distance is maximized. This has shown to reduce the symbol error probability. The relation between *A* and *B* also affects the error probability of the specific bits, which is indicated by (6-19).

The relations between *A* and *B* that maximizes the minimum euclidean distance are $A = \sqrt{2}B$, for BB and BBB, and $A = B$ for BQ. This can be obtained by using the fact that the signal space is $2(M_0+J)$ dimensional.

Figure 6-8 shows the symbol error probability versus the average received energy per bit, $E_b = \frac{\alpha^2(A^2 + JB^2)}{\log_2(M)}$, for the three cases considered. Among these the lowest symbol error probabilities are achieved for the case BBB. BB is better than BQ but there is a loss in bandwidth efficiency. If we add a BPSK signal to BB (we get BBB), then the bandwidth efficiency increases, but the symbol error probability also increases.

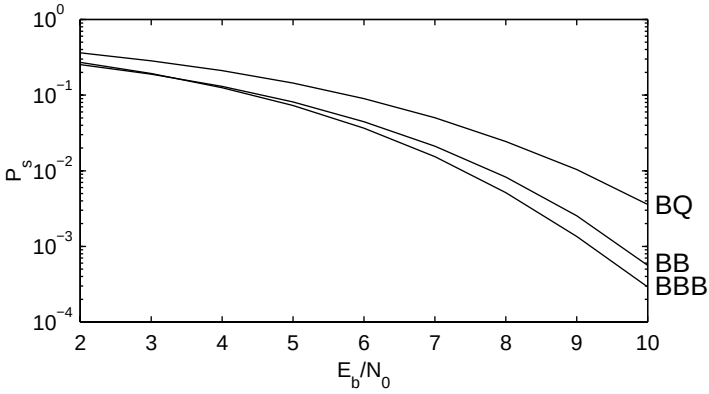

FIGURE 6-8 The symbol error probability for the three systems considered.

Figure 6-9 shows the symbol error probability compared to DPSK and Figure 6-10 shows the symbol error probability compared to non-coherent FSK (NCFSK). The systems are compared with the same number of signal alternatives. The symbol error probabilities for DPSK and FSK are not simulated but calculated, see [41], [51].

Figure 6-9 shows that the symbol error probability for BB is about the same as for 4-DPSK, but at the cost of lower bandwidth efficiency. To increase the bandwidth efficiency BQ can be used. Then there is a loss in energy efficiency but the symbol error probability is better than 8-DPSK. The same is achieved with BBB. The symbol error probability for non-coherent FSK is, in the cases considered, lower than the proposed methods, but the bandwidth efficiency is not as good. We can conclude that the symbol error probability is somewhat between non-coherent FSK and DPSK, and this also holds for the bandwidth efficiency.

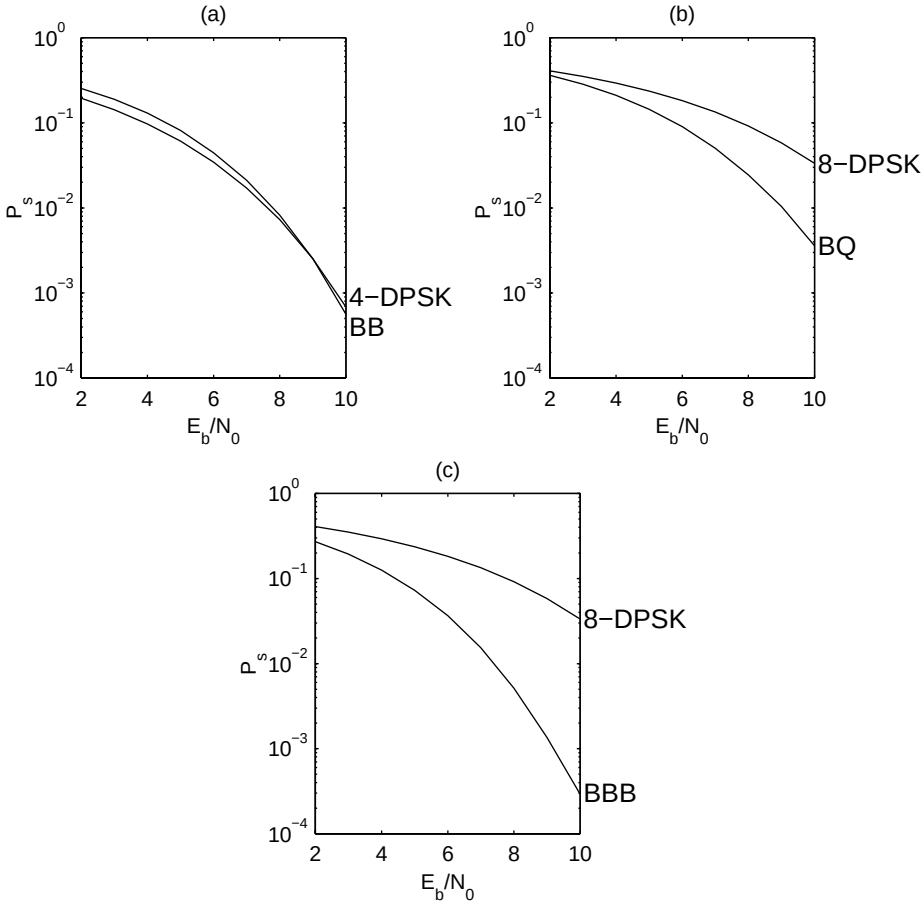

FIGURE 6-9 The symbol error probability compared to DPSK. The methods are compared with the same number of signal alternatives.

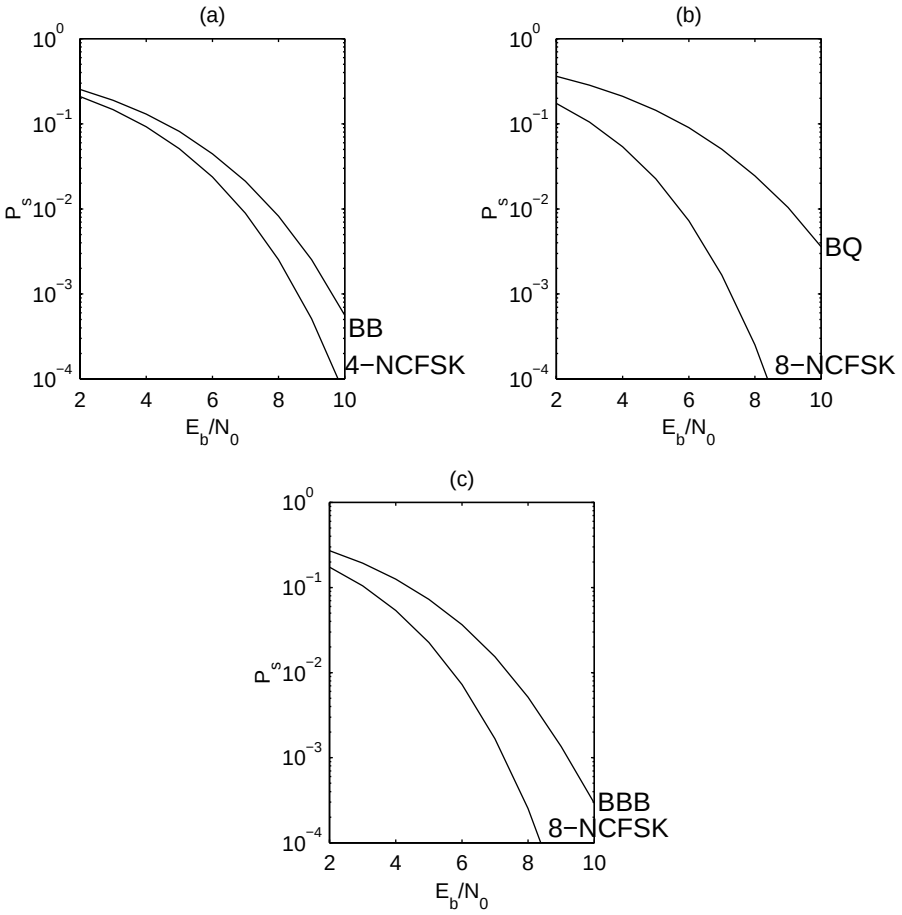

FIGURE 6-10 The symbol error probability compared to non-coherent FSK. The methods are compared with the same number of signal alternatives.

It is clear that it is hard to beat the bandwidth efficiency of DPSK. Additional studies are necessary in order to find competitive alternative signal constellations, when the signals are to be received non-coherently. Furthermore, waveform selection by an appropriate encoder also needs to be investigated.

The relation between *A* and *B* also has to be studied further. Perhaps other constraints than minimizing the euclidean distance could be considered. Also the *J* DPSK signals could have different amplitudes. Here we have considered them as all having amplitude *B*, where *B* is a constant. Because some bits are transmitted as PSK signals and some as FSK signals, different bits can have different error protection.

6.3 Union Bound

The union bound [41] is given by

$$P_s \le \sum_{u=1}^{M} P_u \sum_{\substack{i=1 \\ i \ne u}}^{M} P(C^i > C^u \,|\, m = m_u) \tag{6-20}$$

and is an upper bound on the symbol error probability. P_u is the probability that message u is transmitted and C^u, C^i the metrics for message u and i given in (6-19). In order to calculate the union bound, we have to find the probability $P(C^i > C^u \,|\, m = m_u)$. This probability may also be expressed as

$$P(C^i > C^u \,|\, m = m_u) = P((C^u)^2 < (C^i)^2 \,|\, m = m_u) = P((C^u)^2 - (C^i)^2 < 0 \,|\, m = m_u) \tag{6-21}$$

To arrive at an expression for this probability we first find the distribution of an arbitrary C^l. From (6-19) and (6-10) we obtain

$$\begin{aligned}
C^l &= \left| \sum_{k=1}^{M_0} X_k A_k^l + \sum_{k=1}^{J} Y_k B e^{-j\nu_k^l} \right| \\
&= \left| \sum_{k=1}^{M_0} (\alpha A_k e^{j\theta} + W_k) A_k^l + \sum_{k=1}^{J} \left(\alpha B e^{j\nu_k} e^{j\theta} + W_{k+M_0} \right) B e^{-j\nu_k^l} \right| \\
&= \left| \sum_{k=1}^{M_0} (\alpha A_k^l A_k e^{j\theta} + A_k^l W_k) + \sum_{k=1}^{J} \left(\alpha B e^{-j\nu_k^l} B e^{j\nu_k} e^{j\theta} + B e^{-j\nu_k^l} W_{k+M_0} \right) \right| \\
&= \left| e^{j\theta} \left(\sum_{k=1}^{M_0} (\alpha A_k^l A_k + A_k^l W_k e^{-j\theta}) + \sum_{k=1}^{J} \left(\alpha B^2 e^{j\nu_k - j\nu_k^l} + B e^{-j\nu_k^l} W_{k+M_0} e^{-j\theta} \right) \right) \right| \\
&= \left| \sum_{k=1}^{M_0} (\alpha A_k^l A_k + A_k^l W_k e^{-j\theta}) + \sum_{k=1}^{J} \left(\alpha B^2 e^{j\nu_k - j\nu_k^l} + B W_{k+M_0} e^{-j\nu_k^l} e^{-j\theta} \right) \right| \\
&= \left| \sum_{k=1}^{M_0} \alpha A_k^l A_k + \sum_{k=1}^{M_0} A_k^l W_k e^{-j\theta} + \sum_{k=1}^{J} \alpha B^2 e^{j\nu_k - j\nu_k^l} + \sum_{k=1}^{J} B W_{k+M_0} e^{-j\nu_k^l - j\theta} \right|
\end{aligned} \tag{6-22}$$

Thus there are two constant terms (assuming a given message is sent) and two terms with random variables. The constant part is

$$\sum_{k=1}^{M_0} \alpha A_k^l A_k + \sum_{k=1}^{J} \alpha B^2 e^{jv_k - j\nu_k^l} = \left(\sum_{k=1}^{M_0} \alpha A_k^l A_k + \sum_{k=1}^{J} \alpha B^2 \cos(v_k - \nu_k^l) \right) + j \left(\sum_{k=1}^{J} \alpha B^2 \sin(v_k - \nu_k^l) \right) \tag{6-23}$$

and the random part

$$\begin{aligned}
&\sum_{k=1}^{M_0} A_k^l W_k e^{-j\theta} + \sum_{k=1}^{J} B W_{k+M_0} e^{-j\nu_k^l - j\theta} \\
&= \sum_{k=1}^{M_0} A_k^l W_k \cos(\theta) - j \sum_{k=1}^{M_0} A_k^l W_k \sin(\theta) \\
&+ \sum_{k=1}^{J} B W_{k+M_0} \cos(-\nu_k^l - \theta) + j \sum_{k=1}^{J} B W_{k+M_0} \sin(-\nu_k^l - \theta) \\
&= \sum_{k=1}^{M_0} A_k^l (W_{k,1} + jW_{k,2}) \cos(\theta) - j \sum_{k=1}^{M_0} A_k^l (W_{k,1} + jW_{k,2}) \sin(\theta) \\
&+ \sum_{k=1}^{J} B (W_{k+M_0,1} + jW_{k+M_0,2}) \cos(-\nu_k^l - \theta) \\
&+ j \sum_{k=1}^{J} B (W_{k+M_0,1} + jW_{k+M_0,2}) \sin(-\nu_k^l - \theta)
\end{aligned} \tag{6-24}$$

$$\begin{aligned}
&= \sum_{k=1}^{M_0} A_k^l W_{k,1} \cos(\theta) + \sum_{k=1}^{M_0} A_k^l W_{k,2} \sin(\theta) \\
&+ \sum_{k=1}^{J} B W_{k+M_0,1} \cos(-\nu_k^l - \theta) - \sum_{k=1}^{J} B W_{k+M_0,2} \sin(-\nu_k^l - \theta) \\
&- j \sum_{k=1}^{M_0} A_k^l W_{k,1} \sin(\theta) + j \sum_{k=1}^{M_0} A_k^l W_{k,2} \cos(\theta) \\
&+ j \sum_{k=1}^{J} B W_{k+M_0,2} \cos(-\nu_k^l - \theta) + j \sum_{i=1}^{J} B W_{k+M_0,1} \sin(-\nu_k^l - \theta)
\end{aligned} \tag{6-25}$$

Because $W_{i,j}$ are independent Gaussian random variables with variance $N_0/2$ and zero-mean the variance of the real part in (6-25) is (given θ)

$$\begin{aligned}
&\sum_{k=1}^{M_0} (A_k^l)^2 \frac{N_0}{2} (\cos(\theta))^2 + \sum_{k=1}^{M_0} (A_k^l)^2 \frac{N_0}{2} (\sin(\theta))^2 \\
&+ \sum_{k=1}^{J} B^2 \frac{N_0}{2} (\cos(-\nu_k^l - \theta))^2 + \sum_{i=k}^{J} B^2 \frac{N_0}{2} (\sin(-\nu_k^l - \theta))^2 \\
&= A^2 \frac{N_0}{2} + JB^2 \frac{N_0}{2}
\end{aligned} \tag{6-26}$$

and in the same way the variance of the complex part in (6-25) is

$$\begin{aligned}
&\sum_{k=1}^{M_0} (A_k^l)^2 \frac{N_0}{2} (\cos(\theta))^2 + \sum_{k=1}^{M_0} (A_k^l)^2 \frac{N_0}{2} (\sin(\theta))^2 \\
&+ \sum_{k=1}^{J} B^2 \frac{N_0}{2} (\cos(-\nu_k^l - \theta))^2 + \sum_{k=1}^{J} B^2 \frac{N_0}{2} (\sin(-\nu_k^l - \theta))^2 \\
&= A^2 \frac{N_0}{2} + JB^2 \frac{N_0}{2}
\end{aligned} \tag{6-27}$$

Define the variables X and Y such that

$$\begin{aligned}
|X|^2 &= (C^u)^2 \\
|Y|^2 &= (C^i)^2
\end{aligned} \tag{6-28}$$

Assume message u is transmitted, then X and Y are complex-valued Gaussian random variables (see [41]) with mean

$$\begin{aligned}
\bar{X} &= \left(\sum_{k=1}^{M_0} \alpha A_k^u A_k^u + \sum_{k=1}^{J} \alpha B^2 \cos(\nu_k^u - \nu_k^u) \right) + j \left(\sum_{k=1}^{J} \alpha B^2 \sin(\nu_k^u - \nu_k^u) \right) \\
\bar{Y} &= \left(\sum_{k=1}^{M_0} \alpha A_k^i A_k^u + \sum_{k=1}^{J} \alpha B^2 \cos(\nu_k^u - \nu_k^i) \right) + j \left(\sum_{k=1}^{J} \alpha B^2 \sin(\nu_k^u - \nu_k^i) \right)
\end{aligned} \tag{6-29}$$

The covariance of the random variables X and Y is

$$
\begin{aligned}
\sigma_{XY}^2 &= \frac{1}{2}E\left((X-\bar{X})(Y-\bar{Y})^*\right) \\
&= \frac{1}{2}E\Bigg[\Bigg(\sum_{k=1}^{M_0} A_k^u W_{k,1}\cos(\theta) + \sum_{k=1}^{M_0} A_k^u W_{k,2}\sin(\theta) \\
&+ \sum_{k=1}^{J} BW_{k+M_0,1}\cos\left(-\nu_k^u-\theta\right) - \sum_{k=1}^{J} BW_{k+M_0,2}\sin\left(-\nu_k^u-\theta\right) \\
&+ j\sum_{k=1}^{M_0} A_k^u W_{k,2}\cos(\theta) - j\sum_{k=1}^{M_0} A_k^u W_{k,1}\sin(\theta) \\
&+ j\sum_{k=1}^{J} BW_{k+M_0,2}\cos\left(-\nu_k^u-\theta\right) + j\sum_{k=1}^{J} BW_{k+M_0,1}\sin\left(-\nu_k^u-\theta\right)\Bigg) \\
&\Bigg(\sum_{k=1}^{M_0} A_k^i W_{k,1}\cos(\theta) + \sum_{k=1}^{M_0} A_k^i W_{k,2}\sin(\theta) \\
&+ \sum_{k=1}^{J} BW_{k+M_0,1}\cos\left(-\nu_k^i-\theta\right) - \sum_{k=1}^{J} BW_{k+M_0,2}\sin\left(-\nu_k^i-\theta\right) \\
&- j\sum_{k=1}^{M_0} A_k^i W_{k,2}\cos(\theta) + j\sum_{k=1}^{M_0} A_k^i W_{k,1}\sin(\theta) \\
&- j\sum_{k=1}^{J} BW_{k+M_0,2}\cos\left(-\nu_k^i-\theta\right) - j\sum_{k=1}^{J} BW_{k+M_0,1}\sin\left(-\nu_k^i-\theta\right)\Bigg)\Bigg]
\end{aligned}
\tag{6-30}
$$

Using the fact that the product of two independent zero-mean random processes has zero mean, and the trigonometric identities

$$
\begin{aligned}
\sin(\alpha-\beta) &= \sin\alpha\cos\beta - \cos\alpha\sin\beta \\
\cos(\alpha-\beta) &= \cos\alpha\cos\beta + \sin\alpha\sin\beta
\end{aligned}
\tag{6-31}
$$

we arrive at

$$\sigma_{XY}^2 = \frac{1}{2}E\Big(\sum_{k=1}^{M_0} A_k^u A_k^i W_{k,1}^2 (\cos(\theta))^2 + \sum_{k=1}^{M_0} A_k^u A_k^i W_{k,1}^2 (\sin(\theta))^2$$
$$+ \sum_{k=1}^{M_0} A_k^u A_k^i W_{k,2}^2 (\sin(\theta))^2 + \sum_{k=1}^{M_0} A_k^u A_k^i W_{k,2}^2 (\cos(\theta))^2$$
$$+ \sum_{k=1}^{J} B^2 W_{k+M_0,2}^2 \cos(-\nu_k^u - \theta - (-\nu_k^i - \theta))$$
$$+ j \sum_{k=1}^{J} B^2 W_{k+M_0,2}^2 \sin(-\nu_k^u - \theta - (-\nu_k^i - \theta)) \qquad (6\text{-}32)$$
$$+ \sum_{k=1}^{J} B^2 W_{k+M_0,1}^2 \cos(-\nu_k^u - \theta - (-\nu_k^i - \theta))$$
$$+ j \sum_{k=1}^{J} B^2 W_{k+M_0,1}^2 \sin(-\nu_k^u - \theta - (-\nu_k^i - \theta)) \Big)$$

If we simplify this we get

$$\sigma_{XY}^2 = \frac{1}{2}E\Big(\sum_{k=1}^{M_0} A_k^u A_k^i W_{k,1}^2 + \sum_{k=1}^{M_0} A_k^u A_k^i W_{k,2}^2$$
$$+ \sum_{k=1}^{J} B^2 W_{k+M_0,2}^2 \cos(-\nu_k^u + \nu_k^i) + j \sum_{k=1}^{J} B^2 W_{k+M_0,2}^2 \sin(-\nu_k^u + \nu_k^i) \qquad (6\text{-}33)$$
$$+ \sum_{k=1}^{J} B^2 W_{k+M_0,1}^2 \cos(-\nu_k^u + \nu_k^i) + j \sum_{k=1}^{J} B^2 W_{k+M_0,1}^2 \sin(-\nu_k^u + \nu_k^i) \Big)$$

$$\sigma_{XY}^2 = (\mu_{W^2}) \frac{1}{2}E\Big(\sum_{k=1}^{M_0} A_k^u A_k^i + \sum_{k=1}^{M_0} A_k^u A_k^i + \sum_{k=1}^{J} B^2 \cos(-\nu_k^u + \nu_k^i)$$
$$+ j \sum_{k=1}^{J} B^2 \sin(-\nu_k^u + \nu_k^i) + \sum_{k=1}^{J} B^2 \cos(-\nu_k^u + \nu_k^i) + j \sum_{k=1}^{J} B^2 \sin(-\nu_k^u + \nu_k^i) \Big) \qquad (6\text{-}34)$$

where μ_{W^2} (the mean of $W_{i,j}^2$) is equal to $N_0/2$. The variance of a complex-valued random variable Z is given by

$$\sigma_Z^2 = \frac{1}{2}E((Z - \bar{Z})(Z - \bar{Z})^*) \qquad (6\text{-}35)$$

Similar calculations as above yields the variance of X and Y

$$\sigma_X^2 = \sigma_Y^2 = \mu_{W^2}(A^2 + JB^2) \tag{6-36}$$

This is also seen by setting $i = u$ in (6-34).

Using X and Y the probability $P((C^u)^2 - (C^i)^2 < 0 \,|\, m = m_u)$ may be written as

$$P(|X|^2 - |Y|^2 < 0 \,|\, m = m_u) \tag{6-37}$$

This probability is a special case of a quadratic form given in [41], where it is shown that

$$P(|X|^2 - |Y|^2 < 0 \,|\, m = m_u) = Q_1(a, b) - \frac{v_2/v_1}{1 + v_2/v_1} I_0(ab) \exp\left(-\frac{1}{2}(a^2 + b^2)\right) \tag{6-38}$$

where

$$\begin{aligned}
Q_1(a, b) &= \int_b^\infty x \exp\left(-\frac{1}{2}(x^2 + a^2)\right) I_0(ax) dx \\
a &= \sqrt{\frac{2v_1^2 v_2(\alpha_1 v_2 - \alpha_2)}{(v_1 + v_2)^2}} \\
b &= \sqrt{\frac{2v_1 v_2^2(\alpha_1 v_1 + \alpha_2)}{(v_1 + v_2)^2}} \\
\alpha_1 &= 2(|\bar{X}|^2 \sigma_{YY}^2 + |\bar{Y}|^2 \sigma_{XX}^2 - \bar{X}^* \bar{Y} \sigma_{XY}^2 - \bar{X}\bar{Y}^* (\sigma_{XY}^2)^*) \\
\alpha_2 &= (|\bar{X}|^2 - |\bar{Y}|^2) \\
v_1 &= \sqrt{w^2 + \frac{1}{4(\sigma_{XX}^2 \sigma_{YY}^2 - |\sigma_{XY}^2|^2)}} - w \\
v_2 &= \sqrt{w^2 + \frac{1}{4(\sigma_{XX}^2 \sigma_{YY}^2 - |\sigma_{XY}^2|^2)}} + w \\
w &= \frac{\sigma_{XX}^2 - \sigma_{YY}^2}{4(\sigma_{XX}^2 \sigma_{YY}^2 - |\sigma_{XY}^2|^2)} = 0
\end{aligned} \tag{6-39}$$

$I_0(x)$ is the zeroth-order modified Bessel function of the first kind and $Q_1(x)$ is the generalized Marcum's Q-function.

If we consider (6-20) we see that it is now possible to calculate the union bound. Figure 6-11 - 6-13 show the union bound for each system assuming equally likely signal alternatives. Each figure also shows the simulated symbol error probability. The figures clearly show that, for high signal to noise ratios, the union bound approaches the simulated results.

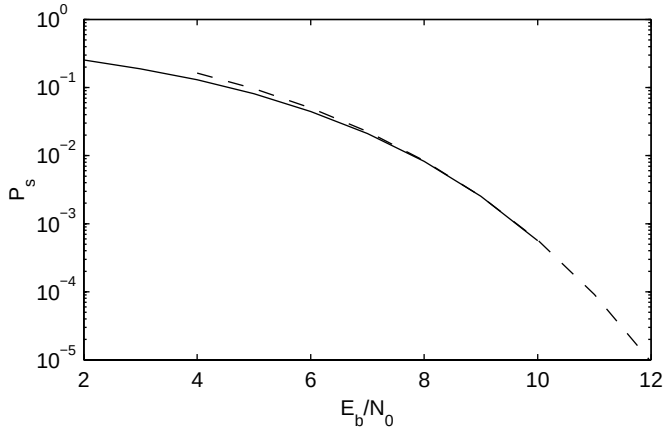

FIGURE 6-11 The union bound of the symbol error probability (the dashed line) and the simulated error probability (the solid line) for BB.

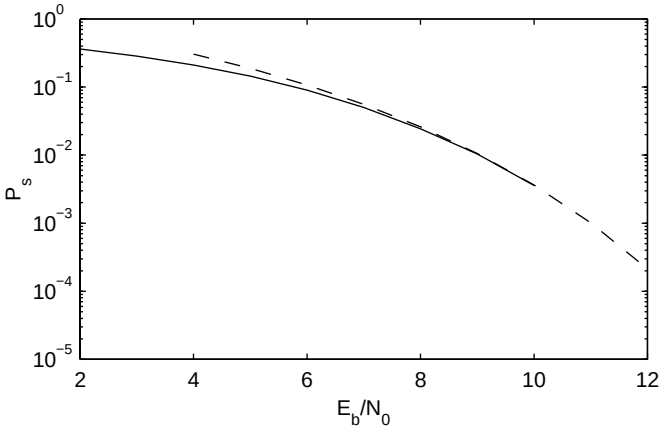

FIGURE 6-12 The union bound of the symbol error probability (the dashed line) and the simulated error probability (the solid line) for BQ.

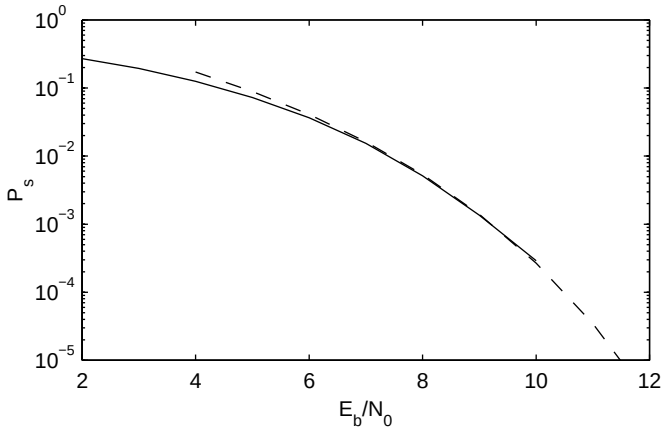

FIGURE 6-13 The union bound of the symbol error probability (the dashed line) and the simulated error probability (the solid line) for BBB.

6.4 Communication Aspects of the Power-Line Communication Channel

In this section we briefly summarize the most important results from this thesis and use them to motivate a structure of a communication system for the power-line channel.

In Chapter 2 and Chapter 3 we study a meter reading system and the results show several parameters that affect the communication in this system. It is shown that the quality of the channels varies in time, physical channel length and with different loads. From these measurements it is already clear that advanced communication methods are needed in order to combat the varying properties of the channel.

Chapter 4 shows measurements of the noise level and the signal attenuation of the power-line channel. The transfer function of the power-line is found to be frequency selective and the magnitude decays with frequency. It is found that the noise is non-white (maybe not even Gaussian), thus it can not be described as AWGN (Additive White Gaussian Noise), which is used to model noise in several communication systems. The power of the noise decays with frequency but there is also a contribution from several narrow-band disturbances.

In Chapter 5 we study the effect of non-white Gaussian noise (narrow-band disturbances) on specific receiver structures and find that if the narrow-band disturbances are not properly dealt with in the receiver, then it can cause a severe degradation in performance. It was also seen that one way to reduce the effects of narrow-band disturbances is to use frequency-diversity.

To communicate on a varying channel like the power-line, a communication method is needed which is able to provide the receiver with large enough signal energy (most of the

time) such that the decision algorithm of the receiver efficiently can combat the disturbances. This can be achieved in several ways. One solution is to let the transmitter and/or the receiver adapt to the channel characteristics. At any time, the characteristics of the channel are estimated and used to change the parameters of the communication system, such that efficient communication is achieved. The complexity of this solution is relatively high and it might be expensive to implement. Another solution is to let the communication system have a robust modulation method that functions well even when the phase and/or the attenuation is unknown. Such a system is less dependent on the channel parameters and, hence, robust communication may be achieved. This is the approach outlined below and is mainly chosen because of the non-complex and less expensive implementation of the receiver.

In this chapter we have studied a modulation method that is a combination of FSK and PSK signals. Because the studied receiver is not dependent on the attenuation of the channel, nor the phase shift, the system is quite robust.

Because the power-line channel is found to be frequency selective it may suggest the use of an OFDM-like (Orthogonal Frequency Division Multiplex) [41], [47] modulation system. In an OFDM system the available bandwidth, *W*, is divided into several small frequency bands, W_1, W_2, ….. W_n, see Figure 6-14. If the bandwidth is divided into small enough sub-bands then the attenuation and the phase shift is approximately constant within each sub-band and, hence, these sub-channels are not frequency-selective. The use of OFDM has also been suggested by other researchers [7], [11], [12], [21], [37].

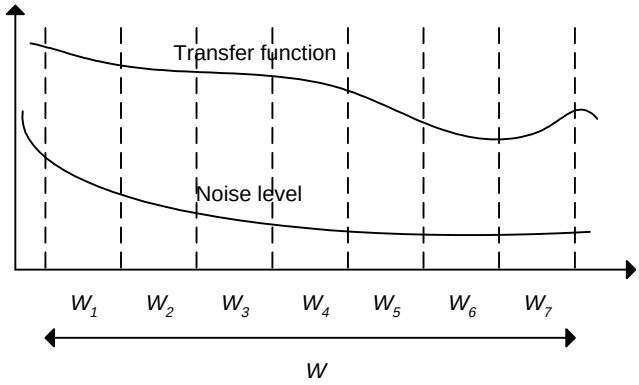

FIGURE 6-14 An example of how the available bandwidth, *W*, is divided into several small sub-bands.

In each sub-band a modulation method is assigned, transmitting bits. Often QAM (Quadrature Amplitude Modulation) signals are used. QAM normally require that the phase and amplitude must be estimated by the receiver. The modulation methods described in this chapter can also be used (combined with proper coding and interleaving). It might be that some sub-bands with known low channel qualities are left unused, e.g., frequency bands containing broadcast radio.

Assume that we assign one BB signal (described in Chapter 6) in each sub-band. This system consists of one BFSK signal and one BPSK signal, thus it transmits two bits each symbol time. If we have n sub-bands then we have n BB systems and the whole communication system transmits $2n$ bits in each symbol interval.

To further increase the performance we could use a convolutional encoder [27] with, e.g., rate 1/2. If bursts of errors exist on the channel then several sequential bits may be lost, and the convolutional encoder might not be able to correct these errors. To try to overcome this impairment an interleaver could be used. An interleaver changes the order of the bits such that they are interleaved in a controlled way. Assume that we have five coded bits $\{a, b, c, d, e\}$ then a simple implementation could be to change the order of the bits such that the new transmitted coded sequence is $\{a, c, e, b, d\}$. Thus, if two sequential bits are lost on the channel then they are not sequential in the original sequence and the decoder might be able to correct the errors.

Figure 6-15 shows a schematic of the whole system. In this example the bandwidth is divided into five sub-bands and in each band a BB signal is used. First the uncoded bit stream is fed to the rate 1/2 convolutional encoder, then the coded sequence is run through the interleaver and the interleaved bit stream is sent to n ($n = 5$) modulators.

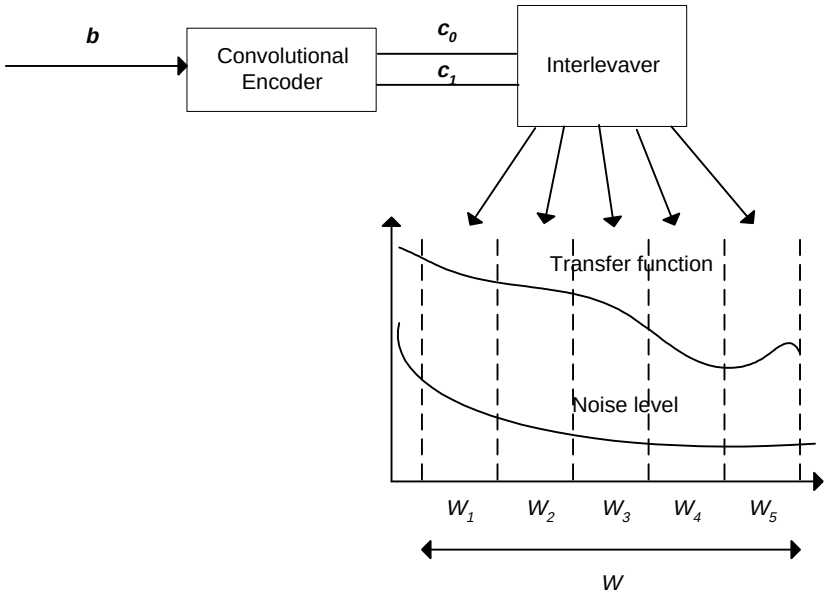

FIGURE 6-15 An example of a communication system for the power-line channel.

Additional research, concerning the system outlined in this section, is needed. Especially important are performance studies, for different choices of encoder, interleaver, modulator and receiver, when communicating over frequency-selective channels.

6.5 Conclusions

In this chapter we have studied a set of modulation methods, which are able to handle unknown phase and attenuation. The reason of doing this is that we want to come up with a communication system with a simple implementation of the receiver. The system consists of one FSK signal and one or more PSK signals, where the FSK signal is used to estimate the received phase for the PSK signals.

It is shown, theoretically and by simulations, that the symbol error probability is higher than for non-coherent FSK and lower than for DPSK, and the same holds for the bandwidth efficiency. This system may be a candidate to be used in power-line communications, but more studies are needed in order to know if the modulation is competitive, especially combined with coding.

This modulation is used combined with coding, frequency diversity and the use of subchannels (similar to Orthogonal Frequency Division Multiplex) to propose a communication system for the power-line channel. The result is a flexible structure which can be upgraded and adapted to future needs.